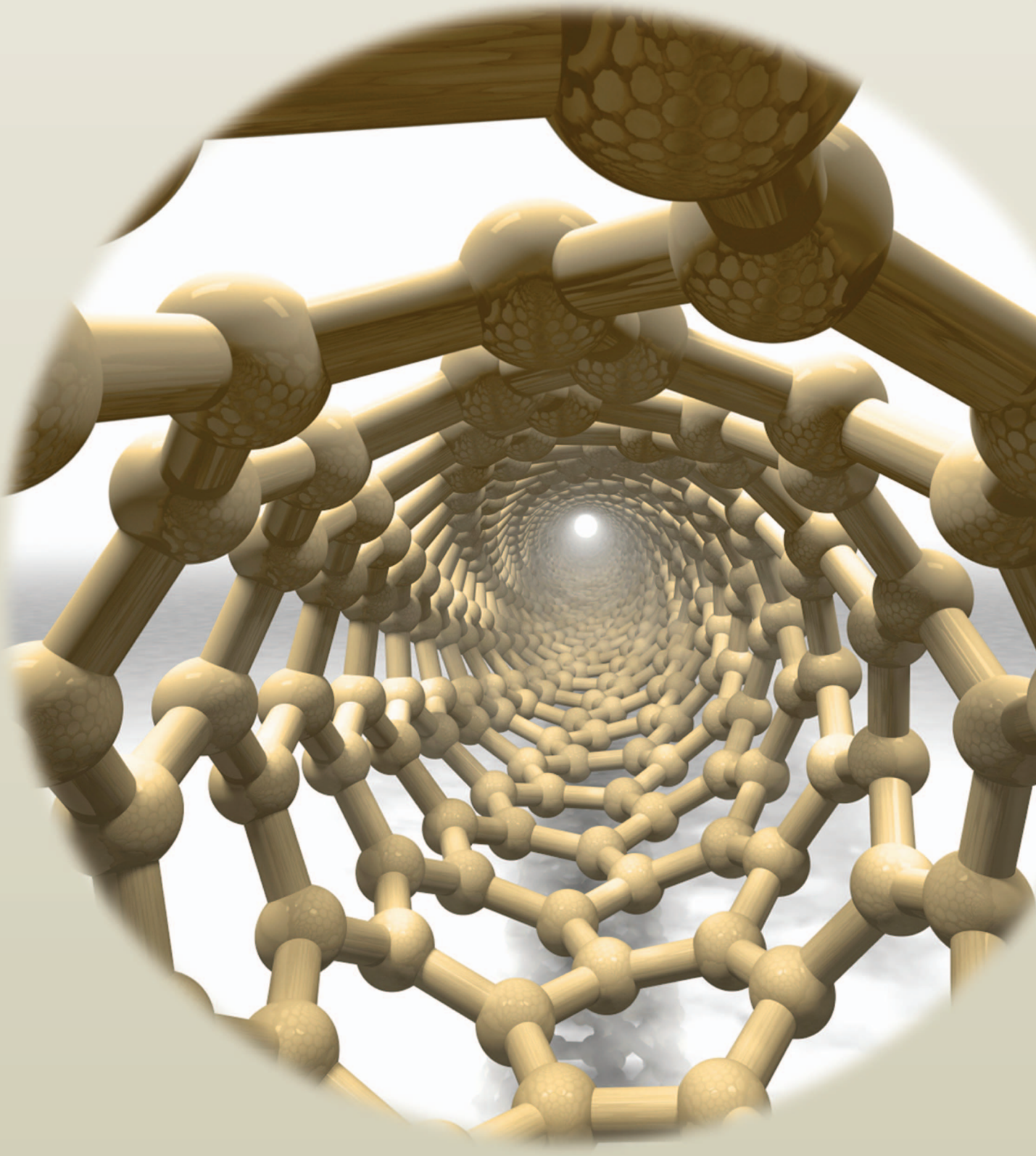

© iSTOCKPHOTO.COM/MARTIN McCARTHY

1527-3342/11/$26.00©2011 IEEE

Nanotechnology Enables Wireless Gas Sensing

Trang T. Thai, Li Yang, Gerald R. DeJean, and Manos M. Tentzeris

Gas sensing is a very important part of everyday life, encompassing applications from engine performance monitoring to chemical plant safety, from climate monitoring to food and health-care applications. In current gas sensing technologies, most gas sensor devices are wired and locally or require some form of integration with a wireless/front-end module that commonly leads to nonportable, increased-cost sensors with limited deployment.

One of the most important applications of such gas sensors involves the ability to monitor the leakage of nitrogen-based gases such as ammonia (NH_3) and nitrogen dioxide (NO_2) in the air because these chemicals adversely affect human and environmental health [5]. NH_3 is primarily a concern in areas of high agricultural activity because it is a natural waste product of livestock whereas it can also be a product of industrial sources, including the manufacturing of basic chemicals, metals, and textile products as well as automotive emissions. High levels of NH_3 can result in irritation to the eyes and respiratory tracts of humans and can negatively impact wildlife, livestock, and agricultural health. NO_2 is also a potentially toxic gas that can lead to respiratory symptoms in humans and detrimentally influence the growth of agriculture. Furthermore, high atmospheric concentrations of either gas can lead to the creation of ground-level smog and acid rain.

There is a tremendous need for real-time, reliable, energy-efficient, and continuous remote gas sensing that would potentially allow for accurate long-term monitoring, enhancing the quality of life. Plus, it has to be stressed that such solutions should be extremely low-cost and scalable to large quantities to enable their straightforward implementation in distributed sensing networks. In this regard, radio frequency (RF) and wireless sensors could be very effective solutions, especially in light of the latest advances in nanotechnology.

An example of a wireless sensor topology at the system level is shown in Figure 1. Although most wireless sensor nodes involve the integration of the sensor circuit with a separate wireless

Trang T. Thai (trang.thai@gatech.edu) and Manos M. Tentzeris (emmanouil.tentzeris@ece.gatech.edu) are with the Georgia Institute of Technology, School of ECE, Atlanta, Georgia 30332, USA; Li Yang (li-yang@ti.com) is with Texas Instruments, Dallas, Texas 75243, USA; Gerald R. DeJean (dejean@microsoft.com) is with Microsoft Research, One Microsoft Way, Redmond, Washington 98052, USA; and Manos M. Tentzeris is a Distinguished Microwave Lecturer of the IEEE MTT-S.

Digital Object Identifier 10.1109/MMM.2011.940594
Date of publication: 5 May 2011

Due to their unique properties, carbon nanotubes have been largely considered one of the most promising materials for next-generation ultrasensitive gas sensors.

module, it would be highly preferable for miniaturization and power-consumption reasons for the sensor itself to be simultaneously a wireless communicating component. That is, it should be able to provide a clear indication of the sensed gas concentration directly in the form of some transmitted or back-scattered wireless signal parameter. Such parameters include the shift of the resonant frequency or the modification of the gain (amount of radiated power) of a sensor-loaded/enabled radiating structure. This would eliminate the need for additional processing circuits and mixed-signal interfaces as well as the need for an external antenna solely serving the purpose of wireless data transmission. The passive implementation of these sensors through the use of power backscattering mechanisms (illumination from a reader and gas-sensitive power reflection from the sensor) would be a further step for significantly reduced power consumption, and thus a lower cost per unit would be provided.

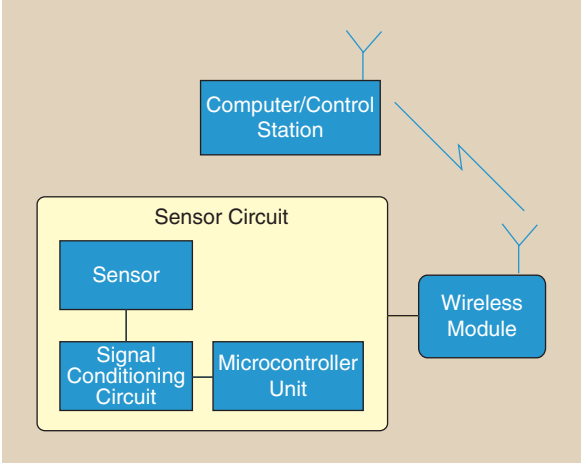

Figure 1. *System-level wireless sensor topology.*

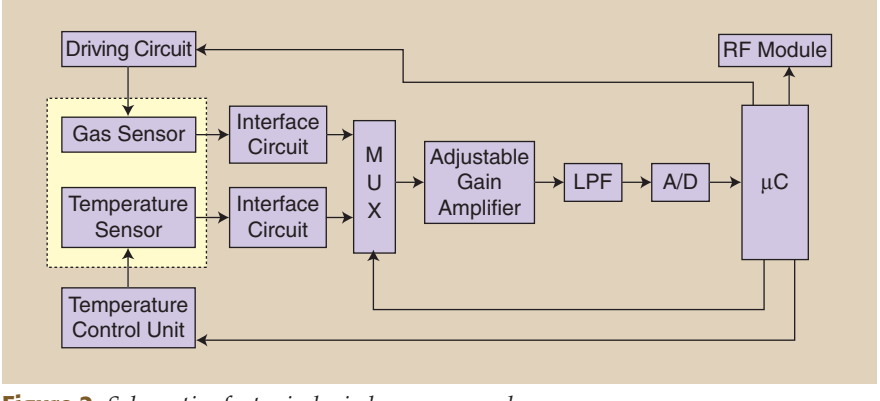

Figure 2. *Schematic of a typical wireless sensor node.*

At the component level, typical wireless/RF gas sensors similar to the schematic shown in Figure 2 can be implemented. The sensing component, also known as a "transducer," transforms the change in gas concentration into the change of an electrical parameter, such as the change of resistance of the sensing structure. This resistance change is subsequently converted to a change in voltage using operational amplifier signal conditioning circuits connected to the microcontroller unit. The signal is then sent to an integrated wireless module/RF front end, such as the Bluetooth module in [14], which utilizes an antenna to communicate with a remote station such as a notebook PC. As is clear from this schematic, the most power-hungry components involve the RF module, the microcontroller (νC), and the amplifier. Ways of eliminating some or even all of these parts without compromising the accuracy and range performance of the sensor would tremendously reduce the power requirements, minimizing battery needs, and allow for truly low-cost implementation.

Most conventional wireless passive sensors suffer from reduced—and many times poor—sensitivity, but recent developments in nanotechnology have opened up new perspectives in this area. Due to their unique properties, carbon nanotubes (CNTs) have been largely considered one of the most promising materials for next-generation ultrasensitive gas sensors. Since their discovery about 20 years ago, CNTs have been a subject of intense investigation and have proven useful in a broad range of applications, especially after the discovery of multiwalled CNTs (MWNTs), which were initially tagged as "helical microtubes of graphitic carbon" by Iijima in 1991 [1]. Although the use of CNTs in practical applications was limited up to 2005 due to issues with fabrication and repeatability, lately they have been used in many domains, ranging from gas sensing and shielding to nanotube-based antennas and RF interconnects [2]–[13]. It has to be stressed that CNT mixtures/composites have been found to have electrical properties highly sensitive to extremely small quantities of gases, such as NH_3, carbon dioxide (CO_2), nitrogen oxide (NO_x), etc., at room temperatures. CNTs have a very fast response time [2], which is a key feature for sensitive gas sensors.

Specifically, CNTs feature characteristics that outperform conventional sensors, including great adsorptive

capacity, due to large surface-area-to-volume ratio, high sensitivity and quick response time resulting in significant changes in electrical properties, such as capacitance or resistance. These features allow material engineering by use of different volume composition ratios (materials with different volume ratios of their composing elements are mixed into a given volume resulting in novel composite materials) [4], and miniaturization. While many types of sensors that utilize the unique properties of CNTs have been proposed, most of them are based on direct contact, where the monitoring station and sensing unit are wired or can be wireless enabled through their integration with a wireless module. The difference between a wireless-enabled sensor and a wireless transducer of a physical parameter is that the former needs a separate RF module with a communication antenna [15], whereas the latter just utilizes the change of one or more microwave/electrical parameters, such as frequency shift, to directly indicate the change of one physical parameter of the environment such as pressure, temperature or gas concentration [3], [16]–[18]. These transducers are passive components, require much simpler processing circuitry, and they need only passive antenna/radiating structures for communication with the exciting reader. In essence, transducers are zero-power implementations since the power they need to activate the sensor is provided by a remote illuminating device.

Despite extensive research in the CNT domain, there has been very limited development of CNT-based wireless transducers [2]–[3], especially in commercial wireless frequency bands due to lack of accurate characterization, effective yield and integrability issues. Although there have been numerous experiments performed on CNT materials, the vast majority of them have taken place at low frequencies or in the optical frequency range. At microwave frequencies, initial efforts include the work of Chopra et al. [3], who demonstrated a disk resonator-based NH_3 sensor that enables remote sensing. In this application, the resonator is coated with CNT composites. The operation is based on the change of the effective relative permittivity of the resonator, which results in a resonant frequency shift of 1–4 MHz when exposed to different gases, including gases such as NH_3, CO_2, and CO at several hundred parts per billion (ppb) to several parts per million (ppm) for a center resonant frequency of 3.889 GHz. Other pioneering efforts in the millimeter frequency range include the work of Dragoman, et al. [19], [20], demonstrating a gas sensor based on a coplanar waveguide (CPW) that measured gas concentration by observing the change in magnitude and phase of the transmission coefficient S_{21} for various gas concentrations.

In this article, we will review various wireless gas sensors operating at microwave frequencies ranging from UHF (500 MHz–1 GHz) to millimeter-wave (20 GHz and above) that demonstrate the unique sensing properties of CNTs over a very broad wireless/RF frequency range. Lower frequencies are commonly used in low-cost RFID-related technologies, while sensors in the millimeter-wave range have the advantage of small size and reduced interference. A specific application of millimeter-wave sensors is for monitoring storage conditions of medicine in hospitals, where there exists significant stray radiation from medical equipment in the low end of microwave range.

Both SWNTs and MWNTs feature ballistic electron transport with no scattering over long distances, thus CNTs can carry high currents with negligible heating.

Properties and Gas Sensing Mechanisms of Carbon Nanotubes

CNTs are graphene sheets that are rolled up in different directions to form an armchair [Figure 3(a)] or zigzag chirality [Figre 3(b)]. In chemistry, chirality refers to a type of molecule that has a nonsuperimposable mirror image. That is, if two molecules are mirror images of one another but they cannot be superimposed, then they are said to have two different chiralities. Similarly, different forms of CNTs are classified based on their chirality. They can be single-walled nanotubes (SWNTs) if the tubes consist of one layer of rolled up graphene, or MWNTs if the tubes have multiple layers of rolled up graphene cylindrical to each other. SWNTs can be either semiconducting or metallic depending on the tube diameter and chirality [22], [23], while MWNTs have only metallic electronic properties. Both SWNTs and MWNTs feature ballistic electron transport with no scattering over long distances, thus CNTs can carry high currents with

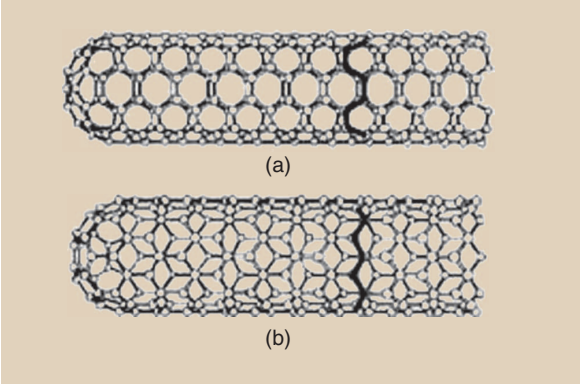

Figure 3. *Illustration of carbon nanotube with (a) armchair chirality and (b) zigzag chirality.*

One of the most distinctive features of the CNTs is their exceptional sensitivity towards extremely small quantities of gases, such as NH_3 and NO_2.

negligible heating [24]. Their lengths range from 1 nm to several hundreds of microns, and, recently, they have been grown to even longer lengths. The properties of CNTs strongly depend on the tube diameter, chirality, and doping. For instance, armchair SWNTs are metallic, while zigzag SWNTs can be either metallic or semiconductive.

One of the most distinctive features of the CNTs is their exceptional sensitivity towards extremely small quantities of gases, such as NH_3 and NO_2. The electrical properties of CNTs are extremely sensitive to charge transfer and chemical doping by various molecules. When electron-withdrawing molecules (e.g., NO_2) or electron-donating molecules (e.g., NH_3) are adsorbed by the semiconducting CNTs, they change the density of the main charge carriers of the nanotube, which effectively modifies the conductivity of the CNT. This behavior forms the basis for applications of CNTs as electrical chemical gas sensors [4]. Detailed studies of gas absorption on CNTs have been carried out, usually by approximate calculations using density functional theory [25]–[29].

RF Principles Utilized in Gas Sensing based on Carbon Nanotubes

Due to the change in electrical properties of CNTs in bundles or in bulk when exposed to different gases, various detection methods have been employed in CNT applications for gas sensing. There exist numerous gas sensors based on individual CNTs, bundles or aligned arrays of CNTs, such as solid-state or surface acoustic wave (SAW) sensors [10]–[16] at dc or low-frequency operation. However, this type of sensor suffers from higher cost and low repeatability, and, usually, a battery is required, leading to mostly active implementations. On the other hand, the development of CNT sensors operating at microwave frequencies, could facilitate the detection of gases since RF parameters, such as scattering parameters and impedance, can be directly monitored based on the gas-sensitive radiation/scattering behavior of CNT materials. In the following, we will consider three different gas sensing methods for microwave applications, all of which rely on self-radiating structures, which allow for simple implementation and passive wireless interrogation.

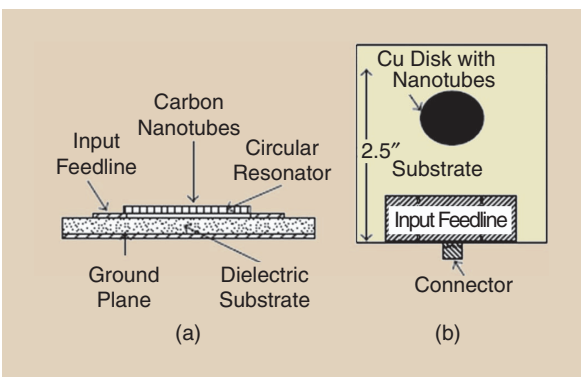

Figure 4. *Disk resonator carbon nanotube-based sensor (a) front view and (b) top view. [3].*

Resonant Frequency Shift Based on a Disk Resonator

Chopra et al. applied SWNTs in powder form on top of a microstrip disk as a thin layer and showed that the resonant frequency of the disk was shifted upon exposure to different gases [3]. The sensor consisted of a circular resonator disk excited by a gap feed microstrip line (Figure 4) and was exposed to gases such as NH_3, carbon monoxide (CO), N_2, helium (He), O_2, and argon (Ar), which altered the dielectric constant of the SWNT coating, thus causing the shift in resonant frequency of the disk. The operation frequencies were around 3 GHz. This system can also be implemented passively, where the coated disk can be interrogated by considering the properties of the reflected signals.

Scattering Parameter Shift of a Coplanar Waveguide

The sensor consists of a CPW and a cavity etched within the substrate of the CPW. A double-wall CNT (DWCNT) mixture was introduced into this cavity as shown in Figure 5 [19], [37]. The CNT-cavity-backed CPW operated at the range of 1–110 GHz. The measurements were performed with CNTs before and after 15 h of exposure to nitrogen gas at the low pressure of 5 bar. A large phase shift of the transmission coefficient (S_{21}) across the operation frequencies was observed after the gas exposure (Figure 6) due to the significant change of the permittivity of the DWNTs that directly modifies the effective permittivity of the CPW transmission line.

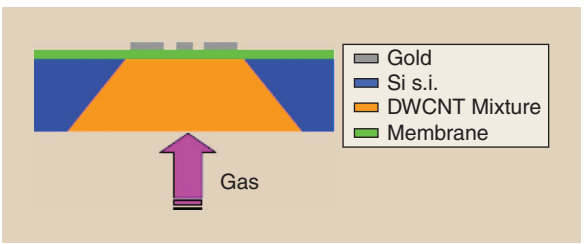

Figure 5. *Carbon nanotube gas sensor based on carbon nanotube, cavity-backed coplanar waveguide [37].*

Wireless CNT-Based Gas Sensor Based on Surface Plasmon Resonance

The combination of CNTs with surface plasmon resonance (SPR) techniques can be used to realize ultrasensitive wireless sensors that can operate in microwave frequencies. Numerous sensors and biosensors have been developed based on optical methods, such as guided modes in optical waveguiding structures (e.g., grating couplers, resonant mirrors) or SPR [38]–[42]. The SPR technique is an optical method for modifying/measuring the refractive index of very thin layers of materials in contact with metals that exhibit large negative real and small positive imaginary dielectric functions [43]–[44]. The utilization of SPR with these materials could enable a very efficient passive, wireless capability for CNT-based gas transducers, linking optics/waveguiding and nanotechnology.

In principle, SPR is a charge-density oscillation that may be excited by incoming electromagnetic waves. The term "plasma" comes from the oscillations of mobile electrons. It exists on the surface of two media with dielectric constants of opposite signs, such as a metal and a dielectric. SPR occurs under the conditions of total internal reflection with p-polarized light [transverse magnetic (TM) polarized waves], in which light polarization has a direction parallel to the plane of incidence. Total internal reflection occurs when a light beam passing through a higher refractive index medium impinges on an interface at a medium of lower refractive index at an angle larger than the so-called critical angle; in this case, the light is totally reflected at the interface. The resonance that occurs when the wave vector of the incident light matches the wavelength of the plasma waves is called "SPR." Incident space waves at radio frequencies can induce surface plasmon waves propagating along the material interface through the use of gratings [45]–[47].

Since surface plasmon waves strongly depend on the interface conditions, their resonance condition is highly sensitive to variations in the electrical

In principle, SPR is a charge-density oscillation that may be excited by incoming electromagnetic waves.

properties of the dielectric adjacent to the metal layer that supports the surface plasmon waves. This approach allows for a passive structure to function as a transducer that can be easily monitored remotely just by monitoring the gas-induced shift of the SPR frequency.

As an example of the coupling of SPR and CNTs, we describe the utilization of CNT mixtures/composites as the dielectric thin-film on an aluminum plate to realize a highly sensitive gas sensor. This sensor's operating principle is based on the excitation of surface plasmons whose resonant frequencies are determined by the air/aluminum/CNT dielectric interface.

The sensor structures are shown in Figures 7 and 8. The dielectric constant values of the CNT thin film are 4.30 and 2.85 at 10 GHz and 60 GHz, respectively [21]. Note that these values were estimated to demonstrate the SPR concept at microwave frequencies through simulations. The objective of this design is to observe the effect of the small gas-induced changes in the dielectric constant of the CNT film on the surface (lossless dielectric) upon the SPR observed in a rectangular grating. Without loss of generality, the CNT dielectric film is set to be lossless, and a change of +2% is applied to the dielectric constant in order to model the reacted sample in the setup shown in Figure 7.

The investigation of SPR on the structure is studied for three cases: aluminum plate covered by dielectric layer with no grating in the absence of gas, aluminum plate covered by dielectric layer with grating before contact with gas, and aluminum plate covered by dielectric layer with grating after contact with gas. The results in Figure 9 [21] for the dielectric layer with a grating show a sharp peak of enhancement around 22 GHz in comparison to the dielectric

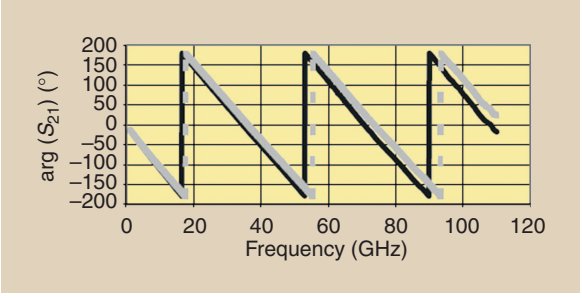

Figure 6. *Phase shift of S_{21} of the carbon nanotube-cavity-backed coplanar waveguide before (black line) and after (gray line) exposure to nitrogen gas.*

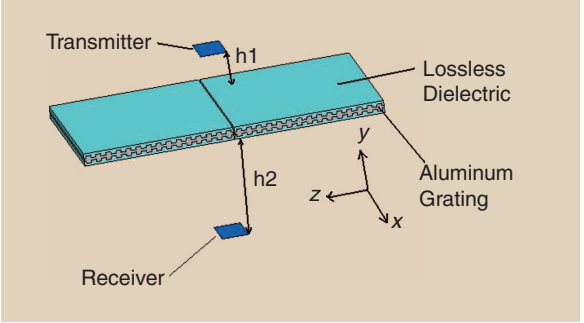

Figure 7. *Carbon nanotube (lossless dielectric) sensing topology utilizing surface plasmon resonance principles [21].*

Over the past few years, there has been an increasing focus on cognitive intelligence wireless applications that aim to couple ambient sensing, identification, communication, and location functions.

layer without a grating (case a in Figure 9) and the dielectric layer with a grating before contact with gas (case b in Figure 9). Before exposure to gas, the enhanced peak is at 22.6 GHz with a magnitude of 0.218. After exposure to gas, the CNT-based dielectric layer experiences a chemical response to the gas that results in a change in its dielectric properties. This causes the peak to shift to 22.2 GHz with a magnitude of 0.208. The frequency shift is about 400 MHz. This result successfully demonstrates the proof-of-concept of the use of SPR for CNT-based gas sensing with an extremely small change (2%) in the dielectric constant of the sensing material. It should be noted that the SPR concept has only been demonstrated with simulations and is given in this review as one of the potential future CNT-based sensitive gas sensing configurations.

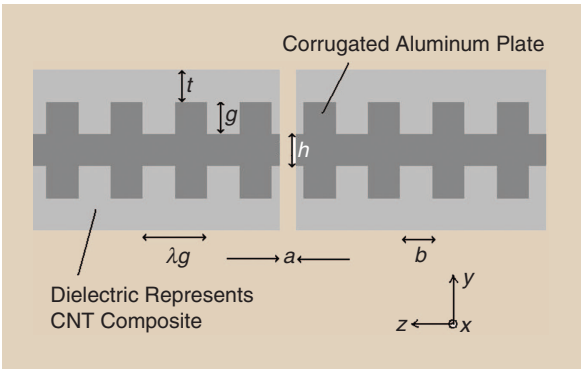

Figure 8. *Cross section of the proposed design incorporating a grating [21].*

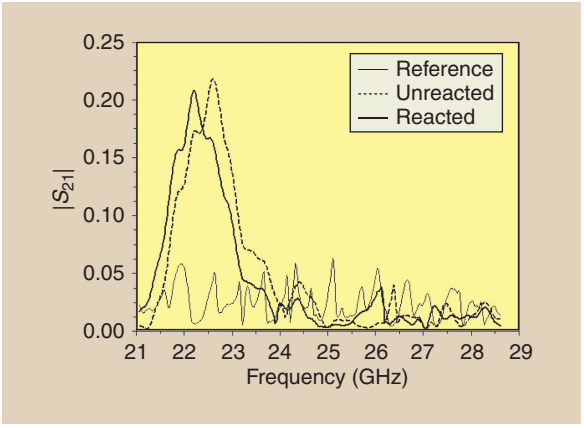

Figure 9. *Simulation results of the magnitude of the transmission coefficient plotted against frequency for (a) the noncorrugated plate covered by dielectric layer before contact with gas, (b) the corrugated plate covered with dielectric layer before contact with gas, and (c) the corrugated plate covered with dielectric layer after contact with gas [21].*

A Success Story: Ink-Jet Printed CNTs in the UHF Range for RFID-Based Ammonia Sensing

Over the past few years, there has been an increasing focus on cognitive intelligence wireless applications that aim to couple ambient sensing, identification, communication, and location functions. One of the manifestations of this trend is the development of wearable electronics, which enable people to effectively wear their personal wireless body-area network (WBAN) that provides medical, lifestyle, assisted living, mobile computing, and tracking functions for the user. Sensing and identification are the key functions of such applications [49]. RF identification (RFID) technologies have provided solutions to such demands. However, integrating conventional sensors on typical RFID [48] organic/paper/plastic flexible substrates utilizing low-cost fabrication processes has been tedious and very limited. Two major challenges for such applications are the choice of the materials and advanced module-level integration capabilities. Previous research has demonstrated the successful development of fully inkjet-printed RFID modules on paper [50]–[51]. Still, most of these efforts lack a discussion of the challenges involved in the integration of practical sensors on these low-cost substrate RFID tags.

From the power consumption aspect, RFID-enabled sensors can be divided into two categories: active and passive. Active RFID-enabled sensor tags use batteries to power their communication circuitry and benefit from a relatively long wireless range. However, the need for an external battery limits their applications only to cases where battery replacement is easy and affordable. Abad et al. has shown various ways to integrate a gas sensor with RFIDs [15], however this approach leads to large-size modules that need to integrate separately the transducer and the antenna. Typical gas sensors utilize materials such as tungsten and zirconium oxides and function on the basis of chemical reactions with the detected gas, which seriously limits their reusability as well as their cost efficiency. Therefore, there has been a growing interest in looking for new materials in RFID sensing applications: ultra-sensitive composites which can be printed directly on the same paper together with the antenna, for a low-cost, flexible, highly integrated RFID-enabled sensing module, requirements the majority of which can be covered by CNTs in a very cost-effective way. Realizing a "multitasking" (sensing/communication) CNT-loaded antenna could

be critical for the realization of practical reduced-size wireless transducers.

Recently, CNT composites have been found to be compatible with inkjet printing [52]. As a direct-write technology, inkjet printing transfers the pattern directly to the substrate. Due to its capability of jetting one single ink droplet in an amount as low as 1 pl, it has widely drawn the attention of the industrial world as a more accurate and economic fabrication method than the traditional lithography method. However, due to the insufficient molecular network formation among the inkjet-printed CNT particles at nanoscale, instabilities have been observed in both the resistance and, especially, the reactance dependence on frequency above several MHz. This limits the CNT applications to dc or the low-frequency bands [53]. To enable the CNT-enabled sensor to be integrated with an RFID antenna at UHF band, a special recipe had to be developed.

Fabrication of Ink-Jet Printed Carbon Nanotubes

To take advantage of the unique gas sensing capabilities of CNTs and integrate them with common inkjet-printed conductive RF passives (for example, antennas), the realization of CNT-based inks is of paramount importance. The SWNTs utilized in a representative sensor module, as discussed in the following, were synthesized from the commonly used electric arc discharge method and are referred to as "AP-SWNTs" [54]. The ratio of semiconducting to metallic SWNTs produced through this method is 2:1. For the preparation of the CNT-based inks, a P3-SWNT type was selected, which is a type of SWNT that has highly dispersible properties in water and other solvents. It was prepared with water for the realization of CNT inks reaching concentrations up to 0.4 mg/ml A high concentration of CNTs in the ink enables successful and durable nanoparticle network formation after printing; otherwise the structure would suffer from an unstable impedance response versus frequency of the SWNT film, such as a sharp drop of the resistance value above 10 MHz. Silver electrodes were patterned

There has been a growing interest in looking for new materials in RFID sensing applications.

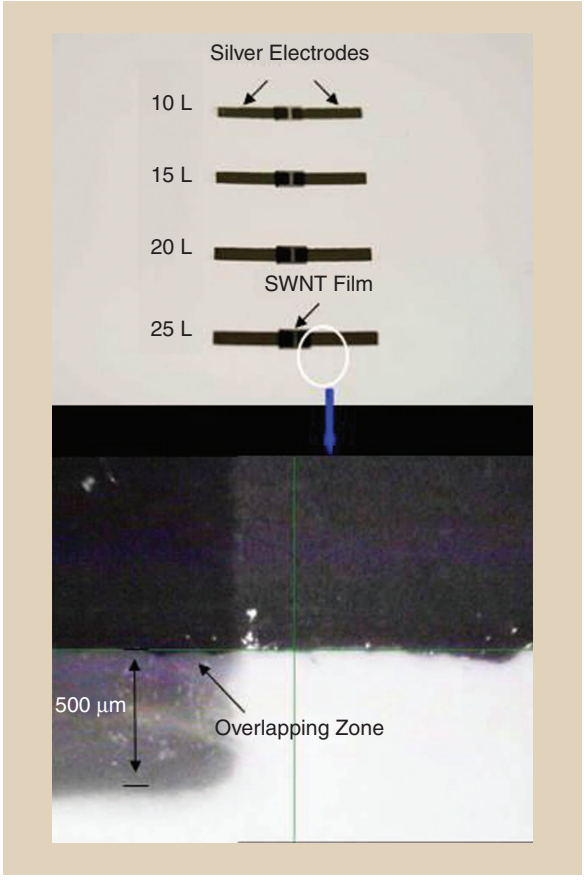

Figure 10. *Photograph of the inkjet-printed single-walled nanotube films with silver electrodes. The number of single-walled nanotube layers of the samples are, from top to bottom, ten, 15, 20, and 25 [16].*

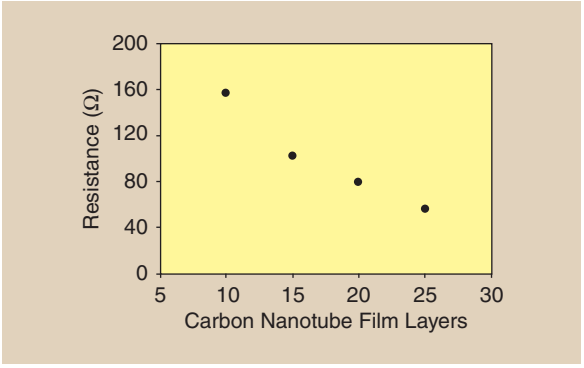

Figure 11. *Measured dc electrical resistance of single-walled nanotube films [16].*

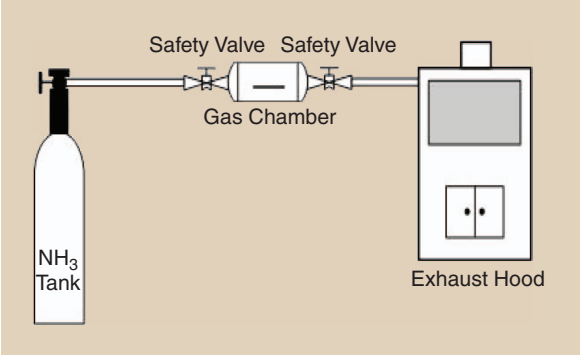

Figure 12. *Schematic of NH_3 gas detection measurement.*

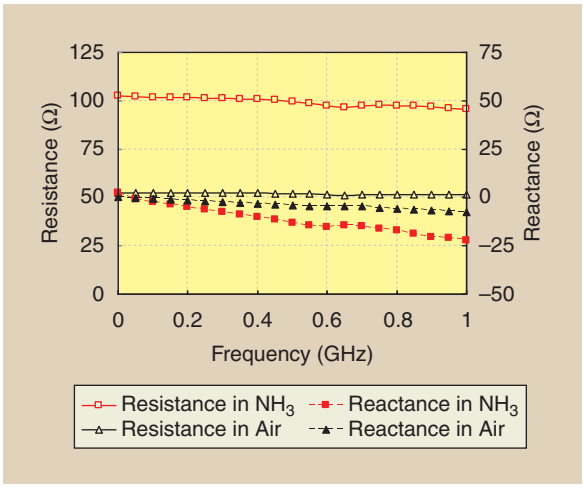

Figure 13. *Measured impedance characteristics of a single-walled carbon nanotube film with 25 layers [16].*

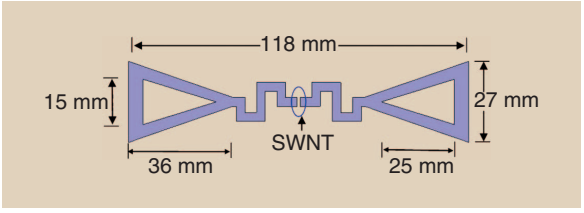

Figure 14. *The RFID tag module designed on a flexible substrate.*

awith conductive ink before depositing the SWNT film. Each printed electrode was 2 × 10 mm, separated by a gap of 0.8 mm. Then, the 3 × 2 mm SWNT film was deposited. The 0.6 mm overlapping zone is to ensure the good contact between the SWNT film and the electrodes. Four devices with ten, 15, 20, and 25 SWNT layers were fabricated to investigate the electrical properties of the film. Figure 10 shows the fabricated samples.

Characterization of Ink-Jet Printed Carbon Nanotubes

The electrical resistance of the SWNT film was measured by probing the end tips of the two electrodes. The dc results are shown in Figure 11. The resistance goes down when the number of SWNT layers increases. Since a high number of SWNT overwritten layers will also help the nanoparticle network formation, the 25-layer film is expected to have the most stable impedance-frequency response and was selected for the gas measurement. In the experiment, 4% consistency NH3, which is widely used in chemical plants, was guided into a 46 cm tube-shape gas-flow chamber connected to an exhaust hood. The test setup is shown in Figure 12. The SWNT film exhibits a fast monotonic impedance response curve to the gas flow.

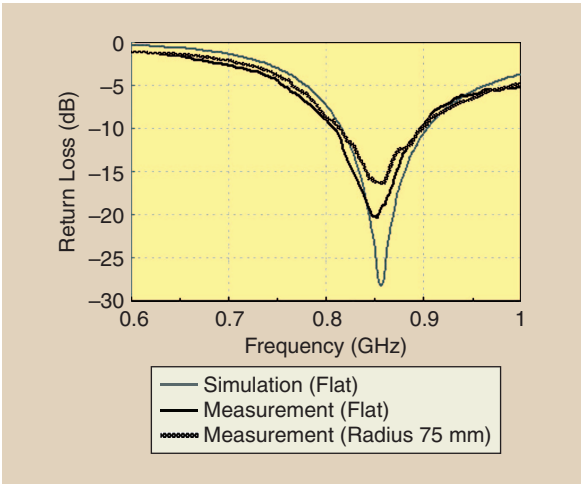

Figure 15. *Simulated and measured return loss of the RFID tag antenna [16].*

A vector network analyzer was used to characterize the SWNT film's electrical performance in the UHF band before and after the gas flow. An RF probe, which is a ground-signal probe, was placed on the silver electrodes for the impedance measurements. The calibration method used was short-open-load-thru (SOLT) with standard coaxial calibration kit. In Figure 13, the gas sensor formed from the SWNT composite having 25 layers shows a very stable impedance response up to 1 GHz, which verifies the effectiveness of the SWNT solvent recipe. At 868 MHz, the sensor exhibits a resistance of 51.6 Ω and a reactance of −j6.1 Ω in air. After NH3 was added to the measurement environment, the resistance was increased to 97.1 Ω, and the reactance was shifted to −j18.8 Ω.

Inkjet-Printed CNT-Loaded RFID-enabled Sensor

The 25-layer SWNT film was next integrated with an RFID tag to form a complete sensor. As described in

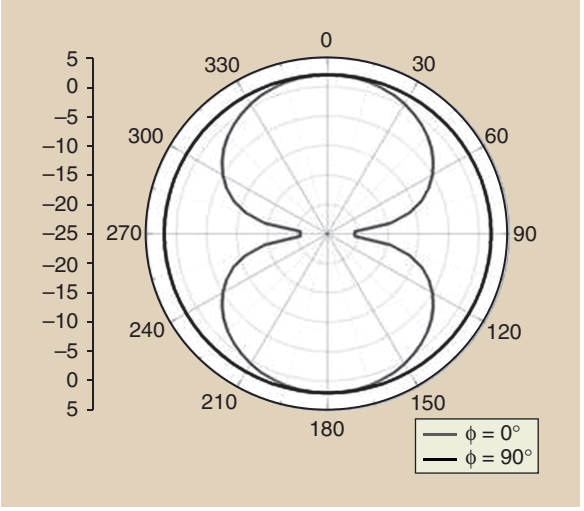

Figure 16. *Far-field radiation pattern plots [16].*

RFID Technology in Sensing Applications

A passive radio-frequency identification (RFID) system operates as follows. The RFID reader sends an interrogating RF signal to the RFID tag consisting of an antenna and an integrated circuit (IC) chip as a load. The IC responds to the reader by varying its input impedance, thus modulating the backscattered signal. The modulation scheme often used in RFID applications is amplitude shift keying (ASK), in which the IC impedance switches between the matched state and the mismatched state [55]. The power reflection coefficient of the RFID antenna can be calculated to evaluate the reflected wave strength

$$\eta = \left| \frac{Z_{\text{load}} - Z_{\text{ANT}}^*}{Z_{\text{load}} + Z_{\text{ANT}}} \right|^2, \tag{S1}$$

where Z_{Load} and Z_{ANT} represent the impedance of the load and the antenna terminals, respectively, with its complex conjugate Z_{ANT}^*.

The same mechanism can be used to realize RFID-enabled sensor modules. The gas-sensing film functions as a tunable resistor, Z_{Load}, with a value determined by the existence of the target gas. The RFID reader monitors the backscattered power level. When the power level changes, it means that there is variation in the load impedance; therefore, the sensor detects the existence of the gas, as illustrated in Figure S1.

The expected power levels of the received signal at the load of the RFID antenna can be calculated using the Friis free-space transmission formula

$$P_{\text{tag}} = P_t G_t G_r \left(\frac{\lambda}{4\pi d} \right)^2, \tag{S2}$$

where P_t is the power fed into the reader antenna, G_t and G_r are the gain of the reader antenna and tag antenna, respectively, and d is the distance between the reader and the tag.

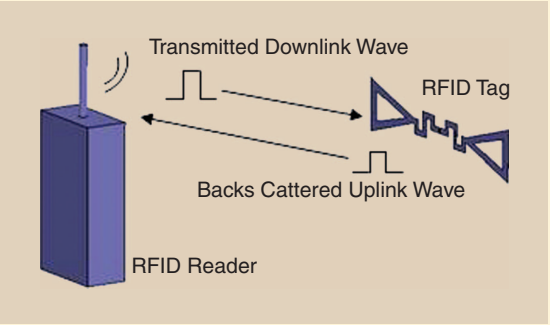

Figure S1. *Conceptual diagram of RFID-enabled sensor modules.*

Due to the mismatch between the sensing material and the tag antenna, a portion of the received power would be reflected back, as in

$$P_{\text{ref}} = P_{\text{tag}} \eta, \tag{S3}$$

where η is the power reflection coefficient in (S1). Hence, the backscattered power received by the RFID reader is defined as

$$P_r = P_{\text{ref}} G_t G_r \eta \left(\frac{\lambda}{4\pi d} \right)^2 = P_t G_t^2 G_r^2 \eta \left(\frac{\lambda}{4\pi d} \right)^4 \tag{S4}$$

or written in decibel form

$$P_r = P_t + 2G_t + 2G_r - 40\log_{10}\left(\frac{4\pi}{\lambda} \right) - 40\log_{10}(d) + \eta, \tag{S5}$$

where all values remain constant before and after the RFID tag is exposed to the gas except η. Therefore, the variation of the backscattered power level solely depends on η, which is determined by the impedance of the gas-sensing film.

"RFID Technology in Sensing Applications," a variation in the backscattered power level is expected when an inkjet-printed SWNT film is used as a load on the RFID tag. To illustrate this power-level change, a bowtie meander line dipole antenna was designed and fabricated on a 100 μm thick flexible paper substrate. The RFID prototype structure is shown in Figure 14 with the SWNT film inkjet printed in the center. The nature of the bowtie shape offers a more broadband operation for the dipole antenna. A dielectric probe station was used for the impedance measurements. The measured Z_{ANT} at 868 MHz is 42.6 +j11.4 Ω.

Simulation and measurement results of the return loss of the CNT-loaded antenna are shown in Figure 15, showing good agreement. The tag bandwidth extends from 810 MHz to 890 MHz, covering the whole European RFID band. The radiation pattern is plotted in Figure 16. It is almost omnidirectional at 868 MHz with directivity around 2.01 dBi and 94.2% radiation efficiency.

In order to verify the performance of the conformal antenna, measurements were performed by sticking the same tag on a 75 mm radius foam cylinder. As shown in Figure 15, there is almost no frequency shifting observed, with a bandwidth extending from 814 MHz to 891 MHz. The directivity is slightly decreased to 1.99 dBi with a 90.3% radiation efficiency. Overall, good performance is maintained with the desired band fully covered. Figure 17 shows the photograph of the designed conformal tag.

In air, the SWNT film exhibited an impedance of 51.6–j6.1 Ω, which results in a power reflection

A variation in the backscattered power level is expected when an inkjet-printed SWNT film is used as a load on the RFID tag.

Figure 17. *Photograph of the conformal tag with a single-walled nanotube film in the center.*

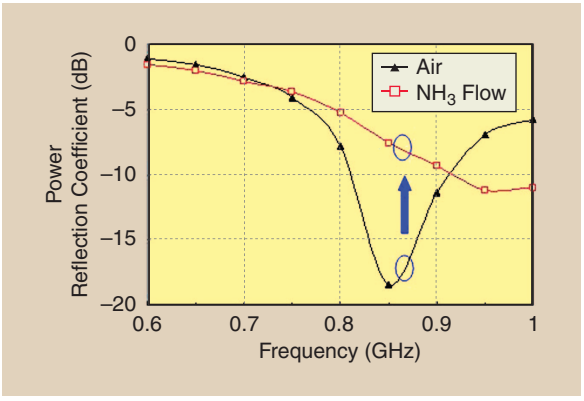

Figure 18. *The power reflection coefficient of the RFID tag antenna with a single-walled nanotube film before and after the gas flow [16].*

of −18.4 dB. When NH_3 is present, the SWNT film's impedance was shifted to 97.1–j18.8 Ω. The mismatch at the antenna port increased the power reflection to −7.6 dB. Using (5), a 10.8 dBi increase at the received backscattered power level was obtained, as shown in Figure 18. By detecting this backscattered power difference on the reader's side, the sensing function can be fulfilled. Although in measurement noise and other issues such as multipath reflection need to be addressed thoroughly, the principle of operation of the CNT-based RFID gas sensor demonstrated here has accomplished a crucial step toward a reality of wearable sensor systems.

Conclusion

Different topologies of CNT-based RF passive gas sensors have been presented, particularly focusing on wireless transducers, which can directly indicate gas concentration through the change of easy-to-monitor RF parameters. CNTs feature numerous unique properties that could potentially enable the next generation of gas sensors with sensitivities better by 1–2 orders of magnitude with respect to existing ones. In addition, CNTs can be easily deposited on conformal and flexible materials utilizing inkjet-printing and other low-cost printing technologies. The CNT-based topologies presented here move the community one step closer to the first truly cognitive generation of smart gas sensors. They also enable the low-cost realization of wearable, real-time gas detection devices with ultralow-power consumption and ultrasensitive selectivity.

References

[1] S. Iijima, *Nature*, vol. 354, pp. 56–58, 1991.

[2] K. G. Ong, K. Zeng, and C. A. Grimes, "A wireless, passive carbon nanotube-based gas sensor," *IEEE Sensors J.*, vol. 2, no. 2, pp. 82–88, 2002.

[3] S. Chopra, A. Pham, J. Gaillard, A. Parker, and A. M. Rao, "Carbon-nanotube-based resonant-circuit sensor for ammonia," *Appl. Phys. Lett.*, vol. 80, no. 24, pp. 4632–4636, 2002.

[4] T. Zhang, S. Mubeen, N. Myung, and M. Deshusses, "Recent progress in carbon nanotube-based gas sensors," *Nanotechnology*, vol. 19, pp. 1–14, July 2008.

[5] D. R. Kauffman and A. Star, "Carbon nanotube gas and vapor sensors," *Nanotechnology*, vol. 47, no. 35, pp. 6550–6570, 2008.

[6] W. Chen, Z. Zhang, Z. Feng, Y. Chen, K. Jiang, S. Fan, and M. Iskander, "Measurement of polarized nano-material (PNM) for microwave applications," in *IEEE MTT-S Int. Microwave Symp. Dig.*, vol. 2, pp. 1577–1580, June 2008.

[7] F. Liu, W. Chen, Z. Zhang, Z. Feng, Y. Chen, and H. Zhang, "Measurement on dipole antenna with light polarized nano-material (PNM) textile reflector," in *IEEE MTT-S Int. Microwave Symp. Dig.*, vol. 2, pp. 1069–1072, June 2009.

[8] T. Thai, J. Ratner, W. Chen, G. DeJean, and M. Tentzeris, "Characterization and testing of novel polarized nanomaterial textiles for ultrasensitive wireless gas sensors," in *Proc. IEEE Electrical Components Tech. Conf.*, 2009, pp. 1049–1052.

[9] G. W. Hanson, "Fundamental transmitting properties of carbon nanotube antennas," *IEEE Trans. Antennas Propagat.*, vol. 53, no. 11, pp. 3426–3435, Nov. 2005.

[10] P. J. Burke, S. Li, and Z. Yu, "Quantitative theory of nanowire and nanotube antenna performance," *IEEE Trans. Nanotechnol.*, vol. 5, no. 4, pp. 314–334, 2006.

[11] P. Burke, C. Rutherglen, and Z. Yu, "Carbon nanotube antennas," in *Proc. SPIE*, 2006, vol. 1, p. 6328.

[12] L. Ying and Z. Baoqing, "Properties of carbon nanotube optical antennae," *Int. J. Infrared Millim. Waves*, vol. 29, no. 10, pp. 990–996, 2008.

[13] K. Jensen, J. Weldon, H. Garcia, and A. Zett, "Nanotube radio," *Nano Lett.*, vol. 7, no. 11, pp. 3508–3511, 2007.

[14] J. K. Abraham, et al., "A compact wireless gas sensor using a carbon nanotube/PMMA thin film chemiresistor," *Smart Mater. Struct.*, vol. 13, no. 5, pp. 1045–1049, 2004.

[15] E. Abada, S. Zampollib, S. Marcoc, A. Scorzonid, B. Mazzolaie, A. Juarrosa, D. Gómeza, I. Elmib, G. C. Cardinalib, J. M. Gómezc, F. Palacioc, M. Cicionid, A. Mondinie, T. Beckerf, and I. Sayhanf, "Flexible tag microlab development: Gas sensors integration in

RFID flexible tags for food logistic," *Sens. Actuators B, Chem.*, vol. 127, no. 1, pp. 2–7, 2007.

[16] L. Yang, R. Zhang, C. P. Wong, and M. M. Tentzeris, "A novel conformal RFID-enabled module utilizing inkjet-printed antennas and carbon nanotubes for gas-detection applications," *IEEE Antennas Wireless Propag. Lett.*, vol. 8, pp. 653–656, June 2009.

[17] T. T. Thai, M. Jatlaoui, H. Aubert, P. Pons, G. R. Dejean, M. M. Tentzeris, and R. Plana, "A novel passive wireless ultrasensitive temperature RF transducer for remote sensing," in *IEEE MTT-S Int. Microwave Symp. Dig.*, Anaheim, CA, June 15–20, 2010, pp. 473–476.

[18] T. T. Thai, G. R. DeJean, and M. M. Tentzeris, "A novel front-end radio frequency pressure transducer based on a millimeter-wave dual-band resonator for wireless sensing," in *IEEE MTT-S Int. Microwave Symp. Dig.*, Boston, MA, June 2009, pp. 1701–1704.

[19] M. Dragoman, K. Grenier, D. Dubuc, L. Bary, R. Plana, E. Fourn, and E. Flahaut, "Millimeter wave carbon nanotube gas sensor," *Appl. Phys. Lett.*, vol. 101, pp. 106103–106104, 2007.

[20] M. Dragoman, K. Grenier, D. Dubuc, L. Bary, E. Fourn, and R. Plana, "Experimental determination of microwave attenuation and electrical permittivity of double-walled carbon nanotubes," *Appl. Phys. Lett.*, vol. 88, no. 15, pp. 153108–153110, 2006.

[21] T. Thai, A. Haque, J. Ratner, M. M. Tentzeris, and G. DeJean, "Development of a fully-integrated ultrasensitive wireless sensor utilizing carbon nanotubes and surface plasmon theory," in *Proc. 2008 IEEE ECTC Symp.*, Orlando, FL, May 2008, pp. 436–439.

[22] B. Q. Wei, R. Vajtai, and P. M. Ajayan, *Appl. Phys. Lett.*, vol. 79, no. 8, pp. 1172–1174, 2001.

[23] M. M. J. Treacy, T. W. Ebbesen, and J. M. Gibson, *Nature*, vol. 381, no. 20, pp. 678–680, 1996.

[24] W. Zhang, Z. Y. Zhu, F. Wang, T. T. Wang, L. T. Sun, and Z. X. Wang, *Nanotechnology*, vol. 15, pp. 936–939, 2004.

[25] S. Peng and K. Cho, "Chemical control of nanotube electronics," *Nanotechnology*, vol. 11, no. 2, pp. 57–60, 2000.

[26] J. Zhao, A. Buldum, J. Han, and J. P. Lu, "Gas molecule adsorption in carbon nanotubes and nanotube bundles," *Nanotechnology*, vol. 13, no. 2, pp. 195–200, 2002.

[27] G. Stan and M. W. Cole, "Hydrogen adsorption in nanotubes," *J. Low Temp. Phys.*, vol. 110, no. 1–2, pp. 539–544, 1998.

[28] C. K. W. Adu, G. U. Sumanasekera, B. K. Pradhan, H. E. Romero, and P. C. Eklund, "Carbon nanotubes: A thermoelectric nanonose," *Chem. Phys. Lett.*, vol. 337, no. 1–3, pp. 31–35, 2001.

[29] H. E. Romero, G. U. Sumanasekera, S. Kishore, and P. C. Eklund, "Effects of adsorption of alcohol and water on the electrical transport of carbon nanotube bundles," *J. Phys. Condens. Matt.*, vol. 16, no. 12, pp. 1939–1949, 2004.

[30] J. Kong, N. R. Franklin, C. Zhou, N. R. Franklin, C. Zhou, M. G. Chapline, S. Peng, K. Cho, and H. Dai, "Nanotube molecular wires as chemical sensors," *Science*, vol. 287, no. 5453, pp. 622–625, 2000.

[31] T. Someya, J. Small, P. Kim, C. Nuckolls, and J. T. Yardley, "Alcohol vapor sensors based on single-walled carbon nanotube field effect transistors," *Nano Lett.*, vol. 3, no. 7, pp. 877–881, 2003.

[32] O. K. Varghese, P. D. Kichambre, D. Gong, K. G. Ong, E. C. Dickey, and C. A. Grimes, "Gas sensing characteristics of multi-wall carbon nanotubes," *Sens. Actuators B, Chem.*, vol. 81, no. 1, pp. 32–41, 2001.

[33] J. Chung, K.-H. Lee, J. Lee, D. Troya, and G. C. Schatz, "Multi-walled carbon nanotubes experiencing electrical breakdown as gas sensors," *Nanotechnology*, vol. 15, no. 11, pp. 1596–1602, 2004.

[34] J. Sippel-Oakley, H. Wang, B. S. Kang, Z. Wu, F. Ren, A. G. Rinzler, and S. J. Pearton, "Carbon nanotube films for room temperature hydrogen sensing," *Nanotechnology*, vol. 16, no. 10, pp. 2218–2221, 2005.

[35] A. Modi, N. Koratkar, E. Lass, B. Wei, and P. M. Ajayan, "Miniaturized gas ionization sensors using carbon nanotubes," *Nature*, vol. 424, no. 6945, pp. 171–174, 2003.

[36] S. J. Kim, "Gas sensors based on Paschen's law using carbon nanotubes as electron emitters," *J. Phys. D, Appl. Phys.*, vol. 39, no. 14, pp. 3026–3029, 2006.

[37] M. Dragoman, A. Muller, D. Neculoiu, G. Konstantinidis, K. Grenier, D. Dubuc, L. Bary, R. Plana, H. Hartnagel, E. Fourn, and E. Flahaut, "Carbon nanotubes-based microwave and millimeter wave sensors," in *Proc. European Microwave Conf.*, 2007, pp. 16–19.

[38] O. S. Wolfbeis, Ed., *Fiber Optic Chemical Sensors and Biosensors*. Boca Raton, FL: CRC Press, 1991.

[39] A. Brecht and G. Gauglitz, "Optical probes and transducers," *Biosensors Bioelectron.*, vol. 10, no. 9–10, pp. 923–936, 1995.

[40] G. Gauglitz, "Opto-chemical and opto-immuno sensors," *Sensor Update,* vol. 1, no. 1, pp. 1–48, Weinheim: VCH Verlagsgesellschaft, 1996.

[41] G. Boisde and A. Harmer, *Chemical and Biochemical Sensing with Optical Fibers and Waveguides*. Boston, MA: Artech House, 1996.

[42] H. Raether, *Surface Plasmons on Smooth and Rough Surfaces and on Gratings*. Berlin: Springer-Verlag, 1988.

[43] R. H. Ritchie, "Plasma losses by fast electrons in thin films," *Phys. Rev.,* vol. 106, no. 5, pp. 874–881, 1957.

[44] K. A. Willets and R. P. Van Duyne, "Localized surface plasmon spectroscopy and sensing," *Annu. Rev. Phys. Chem.*, vol. 58, pp. 267–297, 2007.

[45] A. P. Hibbins, J. R. Sambles, and C. R. Lawrence, "Grating-coupled surface plasmons at microwave frequencies," *J. Appl. Phys.,* vol. 86, no. 4, pp. 1791–1795, Aug. 1999.

[46] J. Homola, I. Koudela, and S. S. Yee, "Surface plasmon resonance sensors based on diffraction gratings and prism couplers: Sensitivity comparison," *Sens. Actuators B, Chem.*, vol. 54, no. 1–2, pp. 16–24, Jan. 1999.

[47] S. S. Akarca-Biyikli, I. Bulu, and E. Ozbay, "Resonant excitation of surface plasmons in one-dimensional metallic grating structures at microwave frequencies," *J. Opt. A, Pure Appl. Opt.*, vol. 7, no. 2, pp. 159–164, 2005.

[48] M. Philipose, J. Smith, B. Jiang, A. Mamishev, S. Roy, K. Sundara-Rajan, "Battery-free wireless identification and sensing," *IEEE Pervasive Comput.*, vol. 4, no. 1, pp. 37–45, 2005.

[49] J. Penders, B. Gyselinckx, R. Vullers, O. Rousseaux, M. Berekovic, M. De Nil, C. V. Hoof, J. Ryckaert, R. F. Yazicioglu, P. Fiorini, and V. Leonov, "Human++: From technology to emerging health monitoring concepts," in *Proc. 5th Int. Summer School and Symp. Medical Devices and Biosensors*, June 2008, pp. 94–98.

[50] L. Yang, A. Rida, R. Vyas, and M. M. Tentzeris, "RFID tag and RF structures on paper substrates using inkjet-printing technology," *IEEE Trans. Microwave Theory Tech.*, vol. 55, no. 12, part 2, pp. 2894–2901, Dec. 2007.

[51] R. Vyas, V. Lakafosis, A. Rida, N. Chaisilwattana, S. Travis, J. Pan, and M. M. Tentzeris, "Paper-based RFID-enabled wireless platforms for sensing applications," *IEEE Trans. Microwave Theory Tech.*, vol. 57, no. 5, part 2, pp. 1370–1382, May 2009.

[52] J. Song, J. Kim, Y. Yoon, B. Choi, and C. Han, "Inkjet printing of single-walled carbon nanotubes and electrical characterization of the line pattern," *Nanotechnology*, vol. 19, no. 9, pp. 1–6, 2008.

[53] M. Dragoman, E. Flahaut, D. Dragoman, M. Ahmad, and R. Plana, "Writing electronic devices on paper with carbon nanotube ink," *Nanotechnology*, vol. 20, no. 37, pp. 1–4, Jan. 2009.

[54] Carbon Solutions, Inc. [Online]. Available: http://www.carbonsolution.com/products/products.html

[55] P. V. Nikitin and K. V. S. Rao, "Performance limitations of passive UHF RFID systems," in *Proc. IEEE Symp. Antennas and Propagation*, July 2006, pp. 1011–1014.